Proceedings of the ECCOMAS Thematic International Conference on Simulation and Modeling of Biological Flows (SIMBIO 2011)
September 21–23, 2011, VUB, Brussels, Belgium

Numerical Simulation of Blood Flow through Insufficient Mitral Valves

Simon J. Sonntag[1]

1 Algorithms & Research, TomTec Imaging Systems
Edisonstrasse 6, 85716 Unterschleissheim, Germany,
simon.sonntag@googlemail.com

Abstract

With the help of Computational Fluid Dynamics (CFD), three-dimensional numerical simulations of blood flow through insufficient mitral valves were performed. The internal fluid domain of the left heart was extracted from MRI images. To simulate the complex flow with rather low Reynolds numbers and a laminar-to-turbulent transition within a reasonable computation time and with high accuracy several mathematical models for turbulence will be examined. The computed velocity field was subsequently scanned in one plane according to a pulsed Doppler echocardiography. With the data collected, 2D colour Doppler images were reconstructed. These images can be directly compared to the computed flow field in order to evaluate Doppler echocardiographic methods for assessing mitral valve dysfunctions. With this approach, various biological as well as technical influences on the imaging of the regurgitation jet, the vena contracta and the proximal isovelocity surface area can be studied in a new manner. In this paper the effect of different spatial resolutions of the ultrasonic transducer will be presented. Furthermore, the turbulent behaviour of the flow with progressively increasing Reynolds numbers will be studied to determine the critical Reynolds number of this specific problem.

Keywords: Computational Fluid Dynamics, Mitral Valve Insufficiency, Blood Flow Simulation, Turbulence Modelling, Large-Eddy Simulation, Colour Doppler Reconstruction, Critical Reynolds Number

Introduction

Heart valve insufficiency is one of the most common cardiovascular diseases. The mitral valve insufficiency is the most frequent variant with a prevalence of 19% in the general population. This results in an enormous relevance for national economies and for public health. The mitral valve is located between the left atrium and the left ventricle of the heart. The valve of patients with mitral insufficiency does not close properly causing a back flow of blood into the left atrium during ventricular systole. Its severity is usually graded on a scale from 1 to 3 (mild, moderate and severe). When it comes to acute mitral insufficiency the regurgitant blood flow leads to a pressure overload of the left atrium, which then increases the pressure in the pulmonary veins. This may cause congestive heart failure and, if untreated, eventually lead to death. Severe mitral regurgitation can be the result of heart abnormalities or another cardiac disease such as rheumatic fever or infective endocarditis [1].

An exact determination of the degree of severity is of great importance in order to achieve an optimal planning and scheduling of the surgical treatment. There are several Doppler echocardiographic methods for assessing mitral valve dysfunctions. Most commonly used in clinical routine are the jet length and jet area methods as well as the assessment of the vena contracta and the proximal isovelocity surface area (PISA). When using the jet-length method, the maximal propagation of the colour Doppler jet is evaluated and analysed. The jet-area method is based on the assessment of the maximal expansion of the jet proportional to the left atrial area. The vena contracta corresponds to the location downstream of the orifice where the cross section of the jet is at a minimum. The diameter of the fluid stream at this location is an indicator for the severity of regurgitant lesions. The PISA region proximal to the mitral valve contains concentric, hemispheric layers of equal velocity. The radius between the orifice and the colour reversal is evaluated and the Gorlin hydraulic formula is applied. The colour reversal is a result of the Nyquist limit, the maximal measureable velocity. As is well known, these echocardiographic methods are severely limited, poorly reproducible and heavily dependent on the examiner [2]. The existing approaches to evaluate the reliability and applicability of these methods, e. g. experiments with flow phantoms [3] or angiographic interventions [4], are, however, limited themselves. The problem is that because of the limitations of the physical measurement process no realistic mapping of the spatial flow field is possible.

In this paper a novel approach for the evaluation of the echocardiographic assessment is presented. The idea is to take the results of CFD computations of the regurgitating blood flow as a basis for the reconstruction of colour

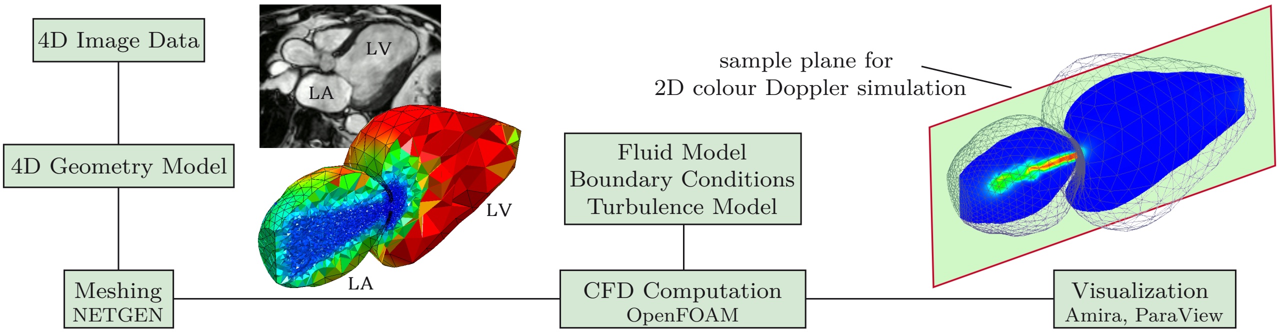

Figure 1 Essential steps and used software for the numerical simulation of blood flow.

Doppler images. These images can be directly compared to the computed flow field in order to evaluate the echocardiographic methods. This approach offers considerable advantages compared to conventional methods.

Numerical Simulation of the Blood Flow

In this section the essential steps and used software for the numerical simulation of blood flow through insufficient mitral valves are discussed. The procedure is also illustrated in Figure 1.

Geometry and Meshing

We extracted the internal fluid domain of the left heart from MRI images (several short-axis and long-axis cuts). Despite an individual and patient-customized geometry of the mitral valve is possible, simple circular pinholes with diameters of 2 mm, 4 mm and 8 mm were used for the three degrees of severity. Therefore, a quantitative comparison between simulation results and analytical results in the literature [5] could be performed. The triangulated surface mesh and the unstructured tetrahedral volume mesh was generated and optimized using the open source mesh generator NETGEN. Geometry based mesh refinement was done in the area of the expected jet and in the proximal convergence zone to a size of $3 \cdot 10^{-4}$ m. The total number of cells was about 0.7 million for the complete mesh. The algorithm of NETGEN is based on an advancing front surface mesh generator, a fast Delaunay algorithm for the volume elements, a back-tracking rule-base algorithm, and a node-movement, element swapping and splitting algorithm for optimization [6].

Fluid Model

The blood was assumed to be homogeneous, viscous, incompressible and Newtonian. From Pedley [7], it is known that the effect of shear forces on the viscosity can be ignored in large vessels without significant loss of accuracy. This refers to using the unsteady 3D Navier-Stokes equations (NSE) as a model for the motion of the fluid:

$$\begin{aligned} \nabla \cdot \boldsymbol{u} &= 0 \\ \frac{\partial \boldsymbol{u}}{\partial t} + (\boldsymbol{u} \cdot \nabla)\boldsymbol{u} + \nabla p - \nu \Delta \boldsymbol{u} &= \boldsymbol{0}, \end{aligned} \tag{1}$$

where $\boldsymbol{u}$ is the flow velocity and p is the pressure. The kinematic viscosity ν of blood was taken as $4.27 \cdot 10^{-6}$ $\mathrm{m^2 \cdot s^{-1}}$ with a density of 1055 $\mathrm{kg \cdot m^{-3}}$ [1].

Initial and Boundary Conditions

Because we had no information about velocities in the heart, initial values of velocity at the boundaries and of the internal field were set to zero. To induce the flow through the mitral valve a fixed total pressure $p_t = p - \frac{1}{2}|\boldsymbol{u}|^2$ was applied at the inlet of the left ventricle and a static pressure was imposed at the outlet of the left atrium. The total pressure boundary condition responds to pressure variations at the inlet because when $\boldsymbol{u}$ changes, p is adjusted accordingly. As in viscous flows the fluid particles stick to solid walls and do not penetrate them, no-slip boundary conditions were specified for the walls of the cardiac chambers.

Turbulence Model

The Reynolds number, which can be considered as a measure for the turbulence intensity of a flow, is defined as

$$\mathrm{Re} = \frac{\text{inertia forces}}{\text{viscous forces}} = \frac{v \cdot D}{\nu}. \tag{2}$$

In this specific problem, v is the maximum amount of orifice velocity, D is the diameter of the orifice and ν is the kinematic viscosity. With a diameter of 2 to 8 mm, a kinematic viscosity of $4.27 \cdot 10^{-6}$ $\mathrm{m^2 \cdot s^{-1}}$ and velocities of about $4 - 6$ $\mathrm{m \cdot s^{-1}}$, this results in a Reynolds number between 1,800 and 10,000. The transition from a laminar condition to a turbulent condition occurs when the Reynolds number exceeded a critical value, the so-called critical Reynolds Number Re_{crit}. Krabill et al [9] and Thomas et al [10] observed experimentally in an in vitro colour Doppler study that the value of Re_{crit} is about 500 for mitral valve regurgitation flows. However, only the more rearwardly located part of the jet is fully turbulent. Studies by Buck et al [11] have shown that in the region of the vena contracta the flow is still laminar. It turned out that the simulation of such a flow with rather low Reynolds numbers and a laminar-to-turbulent transition can be challenging, if high accuracy within a reasonable computation time is desired.

Direct Numerical Simulation (DNS), where no turbulence model is used and all the spatial and temporal scales of the flow have to be resolved, is just suitable for a low Reynolds number flow. In this problem, the Reynolds number is high enough that a very fine mesh and a high temporal resolution are needed, what would require a prohibitively expensive computational effort.

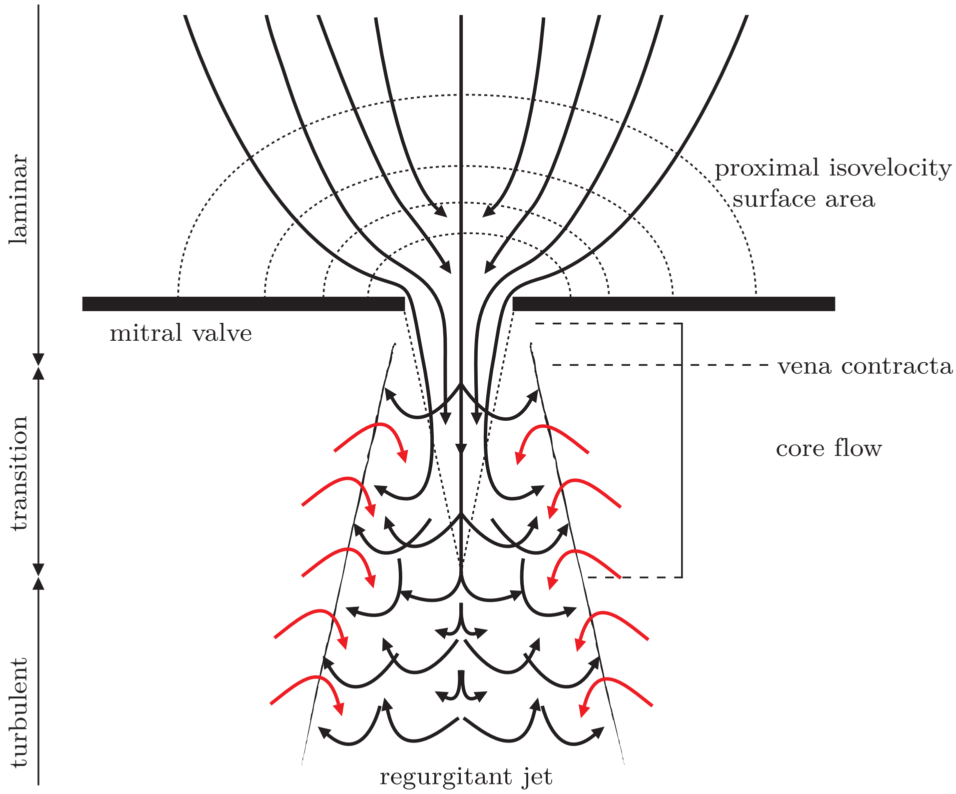

Figure 2 Schematic diagram illustrating the turbulent behaviour of a mitral valve regurgitant flow (based on [8]).

In Reynolds-averaged Navier-Stokes equations (RANS), on the other hand, all of the unsteady fluctuations are averaged out and all the turbulent scales are modelled rather than resolved. This requires a numerical effort much less demanding than DNS, but at the price of accuracy. For all turbulence models tested ($k - \epsilon$, $k - \omega$, SST), we observed a very weak sensitivity to perturbations of the flow what resulted in unphysical solutions. The problem is that these RANS models are mainly suited for fully turbulent flows with high Reynolds numbers [12]. However, because of the transitional nature of the flow and the rather low Reynolds number the flow is anything but fully developed. So this approach is also not suitable for the problem in hand.

The Large-Eddy Simulation (LES), which lies between DNS and RANS, resolves only large, energy-containing scales of the flow, whereas the effect of smaller scales is modelled. The grid itself is used as the filter to separate the large scales from the small ones. The cut-off should lie within the inertial range of the energy spectrum. In contrast to large eddies, which are highly anisotropic and dependent on the geometry and boundary conditions of the specific problem, smaller eddies are self similar, nearly isotropic and have an universal character [13]. These so-called sub-grid scales (SGS) are much easier to model than the large eddies, what is the major benefit of LES over RANS. The computational effort is, however, larger than for RANS, because a considerably finer mesh is necessary. But it is still much less computationally expensive than DNS.

The main task of the SGS model is to dissipate energy at the smallest resolved scales to ensure the right energy transfer through the turbulence spectrum. For this purpose the effective viscosity is increased locally by means of an additional artificial viscosity ν_{SGS} in order to achieve the right dissipation. Here the one equation SGS model proposed by [14] was applied for the sub-grid scale turbulent kinetic energy. The additional transport equation depends on two model parameters, which have an influence on the rate of dissipation and have to be chosen a priori. It turned out that depending on the chosen parameter either too much or too little energy was dissipated locally. The right calibration of the model is very difficult for such a low Reynolds flow, because the inertial range of the energy spectrum is quite small [15]. With the help of a dynamic procedure this drawback could be overcome. Here, the proper model parameters are calculated locally in each timestep based on information contained in the instantaneous resolved scales. So, the right calibration is ensured by changing the value of the parameters. The dynamic procedure, first introduced by [16] for the Smagorinsky model, was extended by Menon and Kim [17] to the one equation model. This localized dynamic kinetic energy model is capable to automatic detect laminar and turbulent regions of the flow and to predict the transition to turbulence time-accurately. For this reason, LES with a dynamic SGS model is the best choice for modelling the complex turbulent flow.

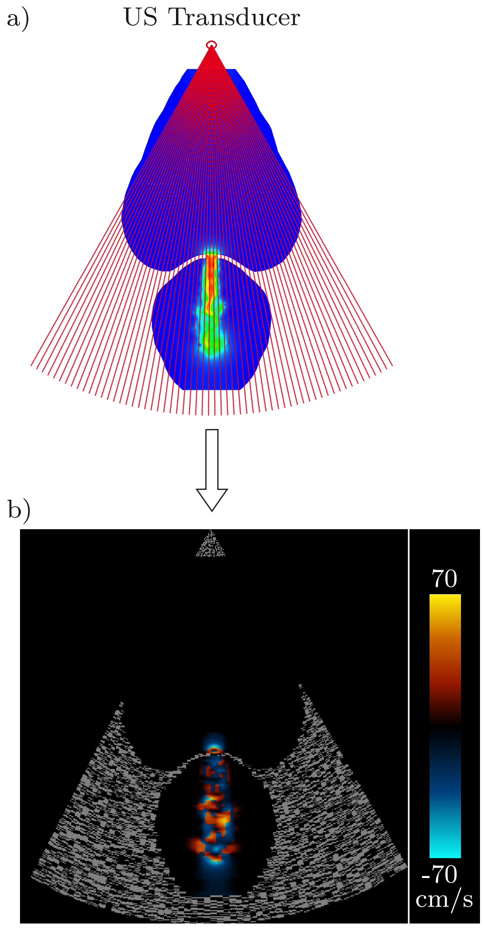

Figure 3 In a) the scanning of the CFD velocity distribution with 60 discrete scan lines and an aperture angle of 60° is illustrated. The result of the subsequent colour Doppler simulation is seen in b).

CFD Computation

In this work, the open source CFD toolbox OpenFOAM has been applied using the finite volume method to numerically solve the system of partial differential equations. To prevent additional artificial dissipation the second order accurate central differencing scheme (CDS) has been applied for the discretization of the spatial terms in the NSE. The use of upwind differencing schemes (UDS) for the spatial discretization of the nonlinear convective term has proven to be inappropriate for performing accurate Large-Eddy Simulations owing to the inherent numerical dissipation of these schemes. It has been shown by Moin et al [18] that even high order UDS still introduce too much artificial dissipation, hence the calibration of the SGS model becomes invalid. A non-dissipative scheme is strongly recommended if using LES. The time derivatives were discretized using the second order accurate and fully implicit three point backward method because of its robustness. Two PISO (Pressure Implicit with Splitting of Operators) loops [19] were used to ensure pressure-velocity coupling. An adaptive time-stepping algorithm was used to maintain a constant maximum courant number of 0.5 in order to ensure a high temporal accuracy and numerical stability.

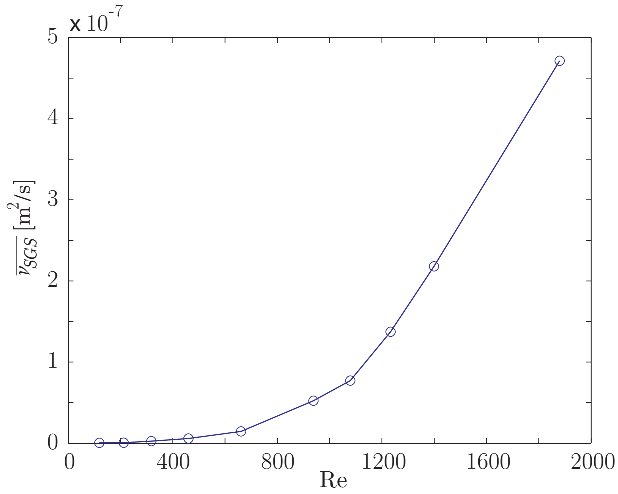

Figure 4 Turbulent behaviour of the flow with progressively increasing Reynolds numbers Re**.** $\overline{\nu_{SGS}}$**, the average of the kinematic SGS viscosity over the whole fluid domain, is indirectly a measure for the turbulence intensity of the flow.**

Colour Doppler Simulation

The computed velocity field was subsequently scanned in one plane according to a pulsed Doppler echocardiography. For this purpose discrete scan lines (ultrasound beams) were emitted from the virtual transducer with an aperture angle of 60°. The position of the virtual transducer was chosen apical in a distance of about 10 cm from the valve opening. This corresponds to the usual distance between the thoracic wall and the mitral valve of grown-ups. The Doppler velocities were determined at 450 equidistantly distributed measure points along each scan line by linearly interpolating the values from neighbouring cell centres. With the data collected, 2D colour Doppler images were reconstructed. For this purpose a MATLAB program was written. A graphical user interface allows the configuration of the Nyquist limit and the baseline shift. The program code consists of: (1) orthogonal projection of the velocity vectors on the scan lines, (2) high pass filter to prevent low-velocity artefact noise and motions at the vascular walls, (3) folding of the velocities about the Nyquist limit over onto the other side of the scale, (4) upsampling to numerically reconstruct the not measured section between two neighbouring scan points, (5) transformation from polar to Cartesian coordinates and (6) colour coding of the Doppler velocities. The result of the colour Doppler simulation is shown in Figure 3b.

Results

The turbulent behaviour of the flow with progressively increasing Reynolds numbers has been studied. Averaging the kinematic SGS viscosity ν_{SGS} over the whole fluid domain, denoted as $\overline{\nu_{SGS}}$, we get indirectly a measure for the turbulence intensity of the flow. In Figure 4 the Reynolds number Re is plotted against $\overline{\nu_{SGS}}$. In order to get higher velocities at the orifice and therefore increasing Reynolds numbers, several simulations with an increasing total pressure from $p_t = 1.5625\ \mathrm{m}^2{\cdot}\mathrm{s}^{-1}$ to $p_t = 10.085$

Table 1 Results of the semi-quantitative echocardiographic methods for different spatial resolutions of the virtual transducer. LA = left atrium.

Scan Lines	**28**	**60**	**120**
Grade I 1/3 2/3 3/3	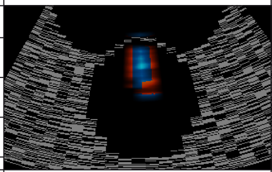	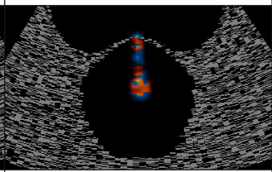	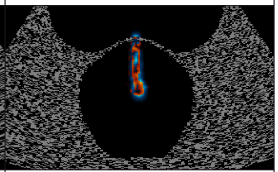
Jet-Length	0.53 LA	0.52 LA	0.51 LA
Jet-Area	0.17 LA	0.09 LA	0.07 LA
Vena Contracta	8.1 mm	3.4 mm	2.2 mm
Grade II 1/3 2/3 3/3	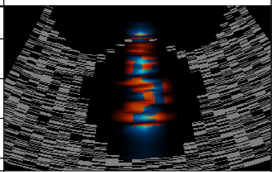	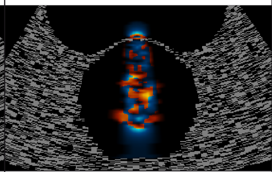	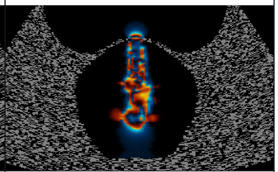
Jet-Length	0.78 LA	0.78 LA	0.79 LA
Jet-Area	0.33 LA	0.25 LA	0.23 LA
Vena Contracta	6.4 mm	4.2 mm	4.0 mm

$m^2 \cdot s^{-1}$ at the inlet were performed. With Reynolds numbers below 300, $\overline{\nu_{SGS}}$ is almost zero. Hence, the flow is laminar. In the Reynolds number range between 300 and 650, $\overline{\nu_{SGS}}$ increases slowly and linearly, what indicates that the flow is transitional. With Re higher than 650, $\overline{\nu_{SGS}}$ increases considerably. The conclusion is that with $\mathrm{Re} > 650$ there are regions of higher turbulence intensity in the flow. Therefore, the critical Reynolds number of $\mathrm{Re}_{crit} = 500$, which was observed experimentally by [9] and [10], is confirmed. Furthermore, the effect of different

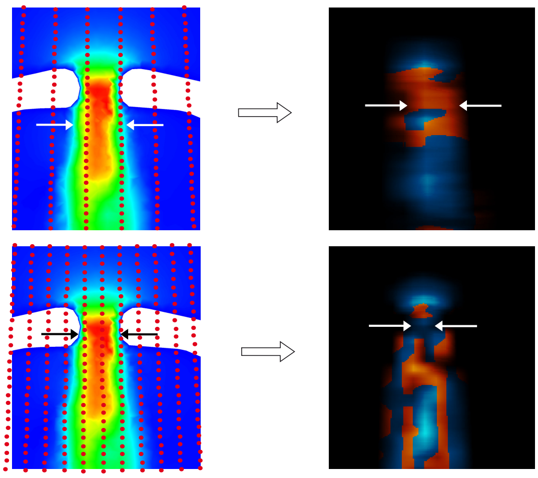

Figure 5 On the left the scanning of the CFD results with a mild severity model is illustrated. The virtual transducer has a spatial resolution of 60 (a) and 120 (b) scan lines in one plane. On the right the results of the corresponding colour Doppler simulations are shown. The arrows indicate the location where the vena contracta would be measured.

spatial resolutions of the virtual transducer on the imaging of the regurgitation jet and the vena contracta were analysed. For this purpose scans with 28 (3D transducer in one plane), 60 and 120 (both 2D transducers) scan lines were performed. In Table 1 the results of the semi-quantitative echocardiographic methods for the mild (I) and moderate (II) grade of mitral valve dysfunction for each of the three resolution settings are listed. In the manner of daily clinical use, the required dimensions and ratios for these methods were measured manually from the simulated colour Doppler images. For comparison of the results with recommended classification criteria we refer to the literature.

It turned out that with a low spatial resolution of the transducer the regurgitation jet is not just imaged inaccurately but also with a wider dimension. This results in a higher ratio between the jet-area and the left atrial area when a 3D transducer is used in comparison to a 2D transducer. When looking at the model with a mild severity, the maximum contraction of the fluid stream is located within the orifice area, conditioned by the geometry of the mitral valve leaflets. Therefore, the vena contracta should be assessed at this location. However, because of the poor spatial resolution the regurgitation jet is not scanned properly in this area with 60 scan lines (Figure 5a). The doctor would measure the vena contracta distal of the orifice (arrows in Figure 5a), where the jet has spread already. The measured value (3.4 mm) would overestimate the severity of the mitral valve dysfunction considerably. When using a high spatial resolution (120 scan lines), the vena contracta is imaged significantly more accurate and can be measured almost correctly (2.2 mm). Hence, the imaging of the vena contracta is strongly dependent on the spatial resolution of the transducer. With a significant degree of severity (grade II), there is a higher reading range in the area of the vena contracta. The jet width can then be measured relatively accurate even at a low spatial resolution of 60 scan lines. With a 3D transducer an accurate measurement is, however, also not possible.

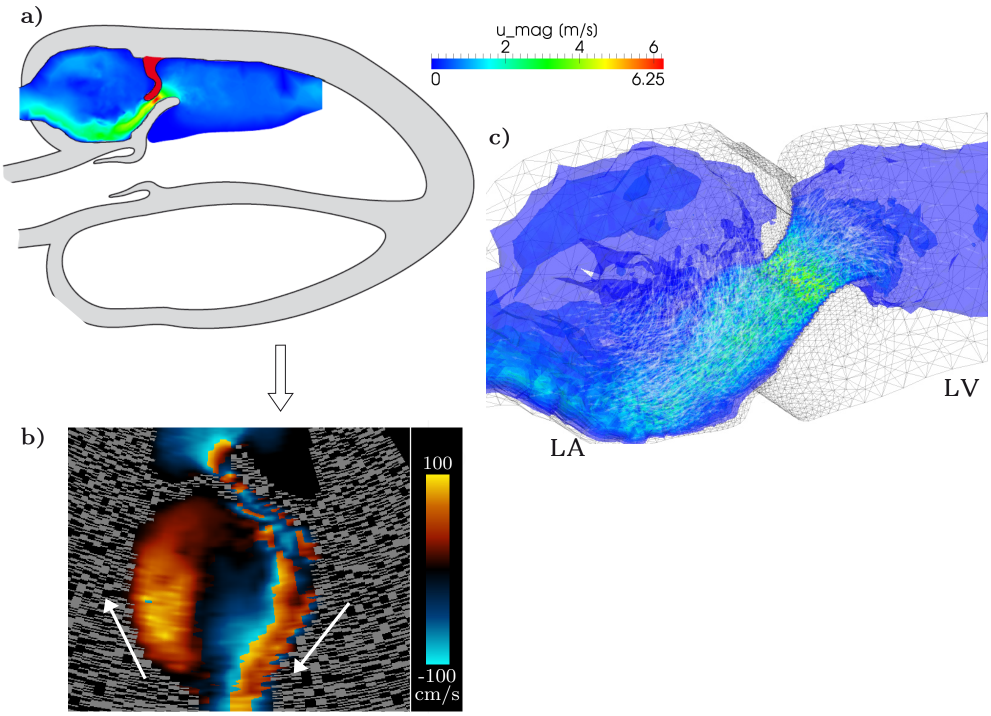

Figure 6 In a) the result of the CFD simulation with a flail leaflet model is shown (backround from [20] with minor modification). The blood flows adhesive along the vascular walls, what results in a rotation of the flow in the left atrium. This can be clearly seen in the according colour Doppler simulation in b). The arrows indicate the direction of the flow. A vector plot with normalised glyphs of the velocity field and three-dimensional contours of the velocity magnitudes $|\boldsymbol{u}| = \pm 0.5$ m/s are shown in Figure c). LA: left atrium, LV: left ventricle.

Discussion and Conclusion

Three-dimensional CFD calculations of blood flow through insufficient mitral valves were performed. It turned out that to time-accurately predict the blood flow through insufficient mitral valves with a laminar-to-turbulent transition and rather low Reynolds numbers between 1,800 and 10,000 can be quite challenging. The Large-Eddy Simulation with a dynamic SGS model proposed by Menon and Kim [17] has proven to be an excellent technique for modelling the complex turbulent flow. This mathematical model is capable to predict all the relevant flow characteristics such as the laminar-to-turbulent transition, the proximal convergence zone, the core flow region and the entrainment. LES with a dynamical model has previously been successfully applied to simulate the transition to turbulent pulsatile blood flow through arterial stenosis, as shown in [12] and [21]. To the best of the author's knowledge, this is the first attempt to simulate the blood flow through insufficient mitral valves using this approach. When using LES it is strongly recommended to use a non-dissipative scheme for the spatial discretization of the convective term of the NSE. Additional artificial dissipation, as is the case when using upwind differencing schemes, makes the calibration of the dynamic SGS model invalid and therefore the computation inaccurate. If there are significant numerical oscillations visible in the solution it is better to use a finer mesh in these regions than using a dissipative scheme.

Furthermore, in this paper we presented an exhaustive study of the turbulent behaviour of the blood flow through insufficient mitral valves. The average of the kinematic SGS viscosity over the whole fluid domain was taken as an indirect measure of the turbulence intensity of the flow and was plotted against progressively increasing Reynolds numbers. With this approach, the critical Reynolds number of $\mathrm{Re}_{crit} = 500$, which was observed experimentally by Krabill et al [9] and Thomas et al [10], could be confirmed.

The computed velocity field was subsequently scanned in one plane according to a pulsed Doppler echocardiography. With the data collected, 2D colour Doppler images were reconstructed. Due to the fact that the CFD results can be analysed exactly, in both qualitative and quantitative terms, a direct comparison with the results of the colour Doppler simulation becomes possible. In contrast to present approaches the reference values are highly accurate and reproducible. Thus, various biological influences, such as the transmitral pressure difference, on the imaging of the regurgitation jet, the vena contracta and the proximal isovelocity surface area can be studied in a new manner. In addition, with the presented procedure it is possible to evaluate different technical specifications and transducer adjustments, for example the colour Doppler imaging of the jet without aliasing or the effect of angular deviation (see [22]). In this paper the differences between 3D and 2D transducers have been presented. It has been shown that the imaging of the vena contracta is strongly dependent on the spatial resolution of the transducer. Such a direct comparison of colour Doppler images and corresponding momentary snapshots of the flow is not possible with existing approaches.

In this study a simple geometry of the mitral valve opening was used. But also more more complex and patient-customized geometries with e. g. adhesive flows along the vascular walls (see Figure 6 and [22]) can be studied non-invasively and without any risk for the patient. Furthermore, besides the presented Doppler echocardiographic methods in this study other methods for assessing mitral valve dysfunctions can be considered. This can also help the development process of new echocardiographic methods. The three dimensional data evaluation of the flow simulation can also give a better understanding and physical insight of the complex flow behaviour of the regurgitating blood. We have to acknowledge that because of the limitations of the physical measurement process the correctness of the CFD calculations could not be validated against experiments. However, the CFD predicted velocity distribution, flow rates and the minimum cross-section at the vena contracta correspond well with literature values [3, 5].

Acknowledgements

The results presented in this paper originate from the author's diploma thesis [22] written under the supervision of Professor O. Junge of the Technical University Munich in cooperation with TomTec Imaging Systems Unterschleissheim. The author thanks Georg Schummers and Marcus Schreckenberg for their supervision at TomTec Imaging Systems.

References

[1] G. Thews, E. Mutschler, and P. Vaupel. *Anatomie, Physiologie, Pathophysiologie des Menschen*. Wissenschaftliche Verlagsgesellschaft mbH, Stuttgart, 4., durchges. edition, 1991.

[2] T. Buck, B. Plicht, R. Wenzel, P. Hunold, and R. Erbel. Echokardiographische Flussquantifizierung zur Schweregradbestimmung von Klappeninsuffizienzen. *Herz*, 27:254–268, 2002.

[3] T. Buck, R. Mucci, J. Guerrero, G. Holmvang, M. Handschumacher, and R. Levine. The power-velocity integral at the vena contracta - a new method for direct quantification of regurgitant volume flow. *Circulation*, 102:1053–1061, 2000.

[4] E. Schwammenthal, C. Chen, F. Benning, M. Block, G. Breithardt, and R. Levine. Dynamics of mitral regurgitant flow and orifice area - physiologic application of the proximal flow convergence method: clinical data and experimental testing. *Circulation*, 90:307–322, 1994.

[5] A. Brucker and et al. *Durchflussmesstechnik*. Oldenbourg, München, 2008.

[6] J. Schöberl. NETGEN An advancing front 2D/3D-mesh generator based on abstract rules. *Comput Visual Sci*, 1(1):41–52, 1997.

[7] T. J. Pedley. *The fluid mechanics of large blood vessels*. Cambridge University Press, Cambridge, 1980.

[8] C. Davies and D. Sahn. Detection and significance of subclinical mitral regurgitation by colour Doppler techniques. *Heart*, 85:369–370, 2001.

[9] K. Krabill, H. Sung, and T. Tamura. Factors influencing the structure and shape of stenotic and regurgitant jets: An in vitro investigation using Doppler color flow mapping and optical flow visualization. *J Am Coll Cardiol*, 13:1672–1681, 1989.

[10] J. Thomas, C. Liu, J. O'Shea, R. Davidoff, S. McGlew, and A. Eeyman. How turbulent is a turbulent jet? An in vitro color flow Doppler study. *J Am Coll Cardiol*, 13:22A, 1989.

[11] T. Buck, B. Plicht, P. Hunold, R. Mucci, R. Erbel, and R. Levine. Broad-beam spectral Doppler sonification of the vena contracta using matrix-array technology - a new solution for semi-automated quantification of mitral regurgitant flow volume and orifice area. *J Am Coll Cardiol*, 45:770–779, 2005.

[12] R. Mittal, S. P. Simmons, and H. S. Udaykumar. Application of Large-Eddy Simulation to the study of pulsatile flow in a modeled arterial stenosis. *J Biomech Eng*, 123:325–332, 2001.

[13] J. H. Ferziger and M. Perić. *Computational Methods for Fluid Dynamics*. Springer Verlag, Berlin, 3. edition, 2002.

[14] A. Yoshizawa and K. Horiuti. A statistically-derived subgrid-scale kinetic energy model for the Large-Eddy Simulation of turbulent flows. *J Phys Soc Jpn*, 54(8):2834–2839, 1985.

[15] N. Liu and X. Lu. Large Eddy Simulation of turbulent concentric annular channel flows. *Int J Numer Meth Fluids*, 45:1317–1338, 2004.

[16] M. Germano, U. Piomelli, P. Moin, and W. Cabot. A dynamic sub-grid-scale eddy viscosity model. *Phys Fluids A*, 3(7):1760–1765, 1991.

[17] S. Menon and W. Kim. Application of the Localized Dynamic Subgrid-Scale Model to Turbulent Wall-Bounded Flows. Technical Report 97-0210, AIAA 35th Aerospace Sciences Meeting, Reno, 1997.

[18] P. Moin and P. Beaudan. Numerical Experiments on the Flow Past a Circular Cylinders at Sub-Critical Reynolds Numbers. Technical Report TF-62, Department of Mechanical Engineering, Stanford University, 1994.

[19] R.I. Issa. Solution of the implicitly discretized fluid flow equations by operator-splitting. *J Comp Physics*, 62:40–65, 1986.

[20] F. A. Flachskampf. *Kursbuch Echokardiografie*. Georg Thieme Verlag KG, Stuttgart, 4. edition, 2009.

[21] M. C. Paul, M. M. Molla, and G. Roditi. Large-Eddy simulation of pulsatile blood flow. *Med Eng Phys*, 31(1):153–159, 2009.

[22] S. J. Sonntag. *Numerische Simulation des Blutflusses an insuffizienten Mitralklappen*. Diploma thesis, Technical University Munich, Faculty for Mathematics. TomTec Imaging Systems, Unterschleissheim., 2010.